



Defense Threat Reduction Agency
8725 John J. Kingman Road, MS 6201
Fort Belvoir, VA 22060-6201



DTRA-TR-12-047

TECHNICAL REPORT

Critical Review of Selected Components of RIPD (Radiation-Induced Performance Decrement)

DISTRIBUTION A: Approved for public release; distribution is unlimited

December 2012

DTRA01-03-D-0014

Authored by:
Terry C. Pellmar
Darren R. Oldson



Prepared by:
Applied Research Associates, Inc.
801 N. Quincy Street
Suite 700
Arlington, VA 22203

THIS PAGE IS INTENTIONALLY LEFT BLANK.

REPORT DOCUMENTATION PAGE				Form Approved OMB No. 0704-0188	
Public reporting burden for this collection of information is estimated to average 1 hour per response, including the time for reviewing instructions, searching existing data sources, gathering and maintaining the data needed, and completing and reviewing this collection of information. Send comments regarding this burden estimate or any other aspect of this collection of information, including suggestions for reducing this burden to Department of Defense, Washington Headquarters Services, Directorate for Information Operations and Reports (0704-0188), 1215 Jefferson Davis Highway, Suite 1204, Arlington, VA 22202-4302. Respondents should be aware that notwithstanding any other provision of law, no person shall be subject to any penalty for failing to comply with a collection of information if it does not display a currently valid OMB control number. PLEASE DO NOT RETURN YOUR FORM TO THE ABOVE ADDRESS.					
1. REPORT DATE (DD-MM-YYYY) 04-12-2012		2. REPORT TYPE Technical Report		3. DATES COVERED (From – To) December 2010 – December 2012	
4. TITLE AND SUBTITLE Critical Review of Selected Components of RIPD (Radiation-Induced Performance Decrement)				5a. CONTRACT NUMBER DTRA-01-03-D-0014-0038	
				5b. GRANT NUMBER	
				5c. PROGRAM ELEMENT NUMBER	
6. AUTHOR(S) Terry C. Pellmar and Darren R. Oldson				5d. PROJECT NUMBER	
				5e. TASK NUMBER	
				5f. WORK UNIT NUMBER	
7. PERFORMING ORGANIZATION NAME(S) AND ADDRESS(ES) Applied Research Associates, Inc. 801 N. Quincy Street, Ste. 700 Arlington, VA 22203				8. PERFORMING ORGANIZATION REPORT NUMBER	
9. SPONSORING / MONITORING AGENCY NAME(S) AND ADDRESS(ES) Defense Threat Reduction Agency 8725 John J. Kingman Road, MS 6201 Fort Belvoir, VA 22060-6201				10. SPONSOR/MONITOR'S ACRONYM(S) DTRA-J9NTSN	
				11. SPONSOR/MONITOR'S REPORT NUMBER(S)	
12. DISTRIBUTION / AVAILABILITY STATEMENT Distribution A: Approved for public release; distribution is unlimited.					
13. SUPPLEMENTARY NOTES					
14. ABSTRACT RIPD (Radiation-Induced Performance Decrement) is a physiologically-based model of acute radiation sickness (ARS). RIPD estimates: <ul style="list-style-type: none"> • severity of illness due to prompt or protracted exposures to ionizing radiation for total free-in-air doses between 0.75 Gy and 45 Gy; • residual performance capability over time for soldiers exposed to ionizing radiation in a military engagement; • incidence of performance decrement; • incidence of lethality; • time to lethality. The RIPD model applies to whole-body exposures to gamma rays and/or neutrons; dose-rate histories can be complex and the exposure period can be as long as one week. RIPD estimates severity of illness and performance capability for up to 1000 hours (about 6 weeks) after the start of exposure. The prompt exposure models in RIPD were developed during the Defense Nuclear Agency's Intermediate Dose Program (IDP) to facilitate consequence assessment and military planning in a nuclear radiation environment. This report (1) summarizes RIPD's performance decrement model, and (2) reviews the four kinetic models around which RIPD's sign/symptom (S/S) severity model structure is built and through which RIPD extends the IDP's prompt exposure S/S severity models to protracted radiation exposures. The assumptions, limitations, and mathematical structure of these four physiologically-based models are discussed.					
15. SUBJECT TERMS					
Radiation Injury		Modeling		Physiological Modeling	
				Performance Decrement	
16. SECURITY CLASSIFICATION OF:			17. LIMITATION OF ABSTRACT	18. NUMBER (of pages)	19a. NAME OF RESPONSIBLE PERSON
a. REPORT UNCLASS			b. ABSTRACT UNCLASS	a. THIS PAGE UNCLASS	UNLIMITED
				42	Paul K. Blake, PhD
					19b. TELEPHONE NUMBER (include area code) 703.767.3433

THIS PAGE IS INTENTIONALLY LEFT BLANK.

UNIT CONVERSION TABLE
U.S. customary units to and from international units of measurement*

U.S. Customary Units	<div> <div>Multiply by </div> <div> Divide by[†]</div> </div>	International Units
Length/Area/Volume		
inch (in)	2.54 $\times 10^{-2}$	meter (m)
foot (ft)	3.048 $\times 10^{-1}$	meter (m)
mile (mi, international)	1.609 344 $\times 10^3$	meter (m)
micron (μ)	1 $\times 10^{-6}$	meter (m)
angstrom (\AA)	1 $\times 10^{-10}$	meter (m)
barn (b)	1 $\times 10^{-28}$	meter ² (m ²)
gallon (gal, U.S. liquid)	3.785 412 $\times 10^{-3}$	meter ³ (m ³)
Mass/Density/Force		
pound (lb)	4.535 924 $\times 10^{-1}$	kilogram (kg)
atomic mass unit (AMU)	1.660 539 $\times 10^{-27}$	kilogram (kg)
pound-mass per cubic foot (lb ft ⁻³)	1.601 846 $\times 10^1$	kilogram per cubic meter (kg m ⁻³)
pound-mass-square foot (lb ft ²)	4.214 011 $\times 10^{-2}$	kilogram-square meter (kg m ²)
pound-force (lbf avoirdupois)	4.448 222	newton (N)
pound-force inch (lbf in)	1.129 848 $\times 10^{-1}$	newton-meter (N m)
pound-force per inch (lbf in ⁻¹)	1.751 268 $\times 10^2$	newton per meter (N m ⁻¹)
Energy/Power		
electronvolt (eV)	1.602 177 $\times 10^{-19}$	joule (J)
Erg	1 $\times 10^{-7}$	joule (J)
kilotons (kT) (TNT equivalent)	4.184 $\times 10^{12}$	joule (J)
British thermal unit (Btu) (thermochemical)	1.054 350 $\times 10^3$	joule (J)
foot-pound-force (ft lbf)	1.355 818	joule (J)
calorie (cal) (thermochemical)	4.184	joule (J)
Pressure		
kip per square inch (ksi)	6.894 757 $\times 10^6$	pascal (Pa)
atmosphere (atm)	1.013 250 $\times 10^5$	pascal (Pa)
Bar	1 $\times 10^5$	pascal (Pa)
torr (Torr)	1.333 224 $\times 10^2$	pascal (Pa)
pound-force per square inch (psi)	6.894 757 $\times 10^3$	pascal (Pa)
Angle/Temperature/Time		
hour (h)	3.6 $\times 10^3$	second (s)
degree of arc (°)	1.745 329 $\times 10^{-2}$	radian (rad)
degree Fahrenheit (°F)	$[T(^{\circ}\text{F}) - 32]/1.8$	degree Celsius (°C)
degree Fahrenheit (°F)	$[T(^{\circ}\text{F}) + 459.67]/1.8$	kelvin (K)
Radiation		
curie (Ci) (activity of radionuclides)	3.7 $\times 10^{10}$	per second (s ^{-1‡})
roentgen (air exposure)	2.579 760 $\times 10^{-4}$	coulomb per kilogram (C kg ⁻¹)
rad (absorbed dose)	1 $\times 10^{-2}$	joule per kilogram (J kg ^{-1**})
rem (equivalent dose)	1 $\times 10^{-2}$	joule per kilogram (J kg ^{-1††})

*Specific details regarding the implementation of SI units may be viewed at <http://www.bipm.org/en/si/>.

†Multiply U.S. customary unit by factor to get international unit. Divide international unit by factor to get U.S. customary unit.

‡The special name for the SI unit of activity of a radionuclide is the becquerel (Bq). (1 Bq = 1 s⁻¹).

**The special name for the SI unit of absorbed dose is the gray (Gy). (1 Gy = 1 J kg⁻¹).

††The special name for the SI unit of equivalent and effective dose is the sievert (Sv). (1 Sv = 1 J kg⁻¹).

THIS PAGE IS INTENTIONALLY LEFT BLANK.

**DTRA-TR-12-047: Critical Review of Selected Components of RIPD
(Radiation-Induced Performance Decrement)**

TABLE OF CONTENTS

List of Figures	viii
List of Tables	viii
Executive Summary	ix
Section 1. Introduction.....	1
1.1 Overview.....	1
Section 2. Determining Performance Decrement	3
2.1 Signs and Symptoms.....	3
2.2 Symptom Profiles and Symptom Complexes	3
2.3 Performance Prediction.....	4
Section 3. Description of Physiologically-Based Models.....	6
3.1 MarCell Model.....	6
3.1.1 Model Description	6
3.1.1.1 <i>Radiation-Induced Cellular Injury</i>	6
3.1.1.2 <i>Probability of Lethality and Calculating the Equivalent Prompt Dose</i>	9
3.1.1.3 <i>Fitting the Parameters</i>	9
3.1.1.4 <i>Calculating Time to Lethality</i>	9
3.1.2 Validation and Limitations	10
3.2 Fatigability and Weakness Model.....	10
3.2.1 Model Description	11
3.2.1.1 <i>Radiation Effects on Lymphocytes</i>	11
3.2.1.2 <i>Cytokine Release</i>	13
3.2.1.3 <i>Severity of Fatigability and Weakness</i>	14
3.2.1.4 <i>Parameter Estimation</i>	15
3.2.2 Validation and Limitations	15
3.3 Upper GI Model.....	16
3.3.1 Model Description	16
3.3.1.1 <i>Emetic Pathway</i>	16
3.3.1.2 <i>Severity of Prodromal Emetic Response</i>	18
3.3.1.3 <i>Parameter Estimation</i>	19
3.3.2 Validation and Limitations	19
3.4 Gut Injury Model	20
3.4.1 Model Description	21
3.4.1.1 <i>Radiation Effects on Cells of the Gut</i>	21
3.4.1.2 <i>Compartmental Model of the Gut Epithelia</i>	23
3.4.1.3 <i>Severity of Lower Gastrointestinal Distress</i>	25
3.4.1.4 <i>Parameter Estimation</i>	26
3.4.2 Validation and Limitations	26
Section 4. Summary and Conclusions	27
Section 5. References.....	28
Appendix A Acronym List	A-1

List of Figures

Figure 1. RIPD's performance decrement calculation.	2
Figure 2. Schematic of MarCell.....	7
Figure 3. Schematic of Lymphopoiesis Model.	11
Figure 4. Schematic of emetic response in UG distress model.....	17
Figure 5. Schematic of the LPL component of the GIM.	20
Figure 6. Schematic of the cellular components in the GIM.	24

List of Tables

Table 1. Marcell model components.....	7
Table 2. Parameters for lymphopoiesis model.....	13
Table 3. Parameters for UG model	19
Table 4. Variables and parameters for the GIM.	20

Executive Summary

The purpose of this report is to provide a concise overview of the physiologically based models in RIPD (Radiation-Induced Performance Decrement), with attention given to the models' mathematical structure and biological assumptions. This report also discusses the use of these models as building blocks for developing models of combined injury.

RIPD is a physiologically-based model of acute radiation sickness (ARS). RIPD estimates:

- severity of illness due to prompt or protracted exposures to ionizing radiation for total free-in-air doses between 0.75 Gy and 45 Gy;
- residual performance capability over time for soldiers exposed to ionizing radiation in a military engagement;
- incidence of performance decrement;
- incidence of lethality;
- time to lethality.

The RIPD model applies to whole-body exposures to gamma rays and/or neutrons; dose-rate histories can be complex and the exposure period can be as long as one week. RIPD estimates severity of illness and performance capability for up to 1000 hours (about 6 weeks) after the start of exposure.

The prompt exposure models in RIPD were developed during the Defense Nuclear Agency's Intermediate Dose Program (IDP) to facilitate consequence assessment and military planning in a nuclear radiation environment. This report (1) summarizes RIPD's performance decrement model, and (2) reviews the four kinetic models around which RIPD's sign/symptom (S/S) severity model structure is built and through which RIPD extends the IDP's prompt exposure S/S severity models to protracted radiation exposures.

RIPD combines physiologically-based and empirical models to predict lethality, time-dependent severity of signs and symptoms, and resulting performance decrement following exposure to ionizing radiation. The approach used to determine performance decrement is briefly detailed, followed by a critical evaluation of the four stand-alone physiological models used by RIPD:

- bone marrow (BM) cell kinetics (MarCell)—basis of RIPD's lethality model and the basis of RIPD's extension (to protracted exposures) of the IDP prompt exposure symptomatology models that reflect bone marrow damage;
- lymphocyte kinetics and subsequent cytokine release – basis of RIPD's extension of the IDP fatigability and weakness (FW) model;
- model of the emetic pathway(s) based on activity of a neuroactive substance – basis of RIPD's extension of the IDP prodromal upper gastrointestinal distress (UG) model; and
- model of cell loss in the intestinal epithelium – basis of RIPD's extension of the IDP lower gastrointestinal distress (LG) model

RIPD is sufficiently versatile to assess anticipated functional incapacitation after exposures to prompt, protracted, and complex exposure histories. RIPD takes into consideration both the prompt gamma and the neutron exposures that would be expected after a nuclear detonation.

Since RIPD was designed for specific military personnel tasks in previous decades, updates reflecting current functions of soldiers and airmen may be warranted. Some of the physiological components could be updated to reflect recent advances in scientific knowledge. Improvements to existing physiological components and addition of new physiological models will allow the program to more accurately assess health risks. New physiologically-based model components will facilitate the integration of treatment as well as other injuries, such as burns, wounds, and infection.

RIPD is the DoD's primary model for prediction of functional impairment after protracted radiation exposures and will serve as a good platform for expansion into new models of health effects and combined injury. With these enhancements, RIPD can evolve into a casualty prediction model that will help military and medical planners predict the incidence of performance incapacitation and health effects, allowing more accurate estimations of time-phased casualties, patient streams, and medical care requirements.

Section 1.

Introduction

1.1 Overview

The purpose of this report is to provide a concise overview of the physiologically based models in RIPD (Radiation-Induced Performance Decrement), with attention given to the models' mathematical structure and biological assumptions. This report also discusses the use of these models as building blocks for developing models of combined injury.

RIPD is a physiologically-based model of acute radiation sickness (ARS). RIPD estimates:

- severity of illness due to prompt or protracted exposures to ionizing radiation for total free-in-air doses between 0.75 Gy and 45 Gy;
- residual performance capability over time for soldiers exposed to ionizing radiation in a military engagement;
- incidence of performance decrement;
- incidence of lethality;
- time to lethality.

The RIPD model applies to whole-body exposures to gamma rays and/or neutrons; dose-rate histories can be complex and the exposure period can be as long as one week. RIPD estimates severity of illness and performance capability for up to 1000 hours (about 6 weeks) after the start of exposure.

RIPD models the performance decrement associated with 23 tasks (generally short-term activities performed during a military engagement). The performance functions calculated by RIPD are intended for consequence assessment and military planning in a nuclear radiation environment.

RIPD's performance decrement calculation is a two-step process, illustrated in Fig. 1-1. Development of mapping ① (Baum *et al.* 1984, Anno *et al.* 1985, Anno *et al.* 1989) and mapping ② (Anno *et al.* 1984, Anno *et al.* 1994) was initiated during the Defense Nuclear Agency's Intermediate Dose Program (IDP). In this early stage of development the domain of function ① was restricted to prompt exposures (empirical data were available to predict severity of signs and symptoms (S/S) for acute doses of radiation; data for the symptomatology elicited by protracted exposures were sparse). Using physiologically-based models, RIPD is able to predict consequences resulting from complex exposure histories that include prompt, protracted, and/or fractionated exposures. That is, RIPD extends mapping ① in Fig. 1-1 to include protracted exposures (Anno *et al.* 1991, Anno *et al.* 1996).

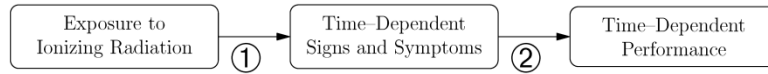


Figure 1. RIPD's performance decrement calculation.

RIPD uses a quantitative description of the sign/symptom severities of ARS developed by the IDP in the early 1980s. The IDP methodology divides the major signs and symptoms (S/S) of ARS into six categories (Young and Auton 1984, Anno *et al.* 1996): upper gastrointestinal distress (UG), fatigability and weakness (FW), lower gastrointestinal distress (LG), hypotension (HY), infection and bleeding (IB), and fluid loss and electrolyte imbalance (FL). Models of the incidence and severity of these symptoms together with a model of hematopoietic lethality form the basis of RIPD.

In addition to empirical models for manifest UG distress, FL, IB, and HY, RIPD includes four physiologically-based models:

- bone marrow (BM) cell kinetics (MarCell) – basis of RIPD's lethality model and the basis of RIPD's extension (to protracted exposures) of the IDP prompt exposure symptomatology models that reflect bone marrow damage;
- lymphocyte kinetics and subsequent cytokine release – basis of RIPD's extension of the IDP fatigability and weakness (FW) model;
- model of the emetic pathway(s) based on activity of a neuroactive substance – basis of RIPD's extension of the IDP prodromal UG distress model; and
- model of cell loss in the intestinal epithelium – basis of RIPD's extension of the IDP lower gastrointestinal distress (LG) model

These physiologically-based models build on a broad base of scientific investigations into the cellular, physiological, and behavioral effects of radiation in biological systems. The general approach used by RIPD is to combine animal experiments and any available human data to model physiological cascades of events initiated by radiation insults. An advantage of modeling these radiation-induced changes using physiologically-based models is that one can define physiologically-based isoeffects.¹ Given prompt-dose experimental data, these isoeffects can be used to estimate the effects of protracted exposures. An isoeffect can be used to determine an equivalent prompt dose, and from a probit analysis of the human dose-response relationship for acute exposures, biological effects could be predicted for complex exposure paradigms.

The following sections (1) summarize RIPD's performance decrement model, and (2) review the four kinetic models around which RIPD's S/S severity model structure is built and through which RIPD extends the IDP's prompt exposure S/S severity models to protracted radiation exposures.

¹ By isoeffect we mean a specific endpoint within the model (e.g., nadir of a cell population) that is predictive of the extent of the damage (e.g., probability of lethality) and can be determined for any radiation exposure scenario. For example, in the MarCell model, the nadir of a bone marrow cell population is assumed to be an isoeffect for probability of lethality. Given the cell population nadir associated with a complex exposure scenario (where lethality could be hard to predict), one can calculate an equivalent prompt dose with which to predict lethality.

Section 2.

Determining Performance Decrement

2.1 Signs and Symptoms

RIPD estimates severity of illness and performance capability for up to 1000 hours (about 6 weeks) after the start of exposure. Prodromal symptoms appear within the first few hours to days following the start of exposure; these symptoms include nausea, vomiting, anorexia, diarrhea, fluid loss, electrolyte imbalance, headache, and fatigability and weakness. Manifest illness occurs a few days to weeks after exposure. During the manifest illness phase, damage to the hematopoietic system triggers infection, fever, and bleeding; ulceration and damage to the gastrointestinal system causes fluid loss, electrolyte imbalance, and recurrence of diarrhea with relatively high doses. To quantify the severity of the signs and symptoms, RIPD uses six S/S categories:

1. upper gastrointestinal distress,
2. lower gastrointestinal distress,
3. fatigability and weakness,
4. hypotension,
5. infection, bleeding, and fever,
6. fluid loss and electrolyte imbalance.

These six categories were chosen because they were commonly addressed in the literature as sequelae of radiation injury, the symptomatology in these six categories spanned a large range of time and radiation dose, and the levels of severity could be described fairly easily (Anno *et al.* 1985).

2.2 Symptom Profiles and Symptom Complexes

Data on the onset, duration, incidence, and severity of the S/S were obtained primarily from case studies of the victims of radiation accidents and records of radiation therapy patients (Anno *et al.* 1989, Baum *et al.* 1984). The symptomatology reported in numerous sources was grouped into 8 dose ranges over the range of interest (0.75 to 45 Gy free-in-air). For each symptom and dose range, time-severity response profiles were constructed (Anno *et al.* 1989, 1996, Baum *et al.* 1984). When the data from accidents and therapy were inadequate, expert opinion was sought to fill the gaps (Anno *et al.* 1989).

- The relationship between the time course (onset and duration) of prodromal symptoms and radiation dose was best-fit with linear regression analysis.
- The “incidence” of any particular symptom (at a specified dose level and a defined severity) is its likelihood of occurrence within the population. A dose-response relationship for the incidence of each symptom was constructed from maximum-likelihood probit analyses of the empirical data (Anno *et al.* 1989, Anno *et al.* 1992, and in Anno *et al.* 1996 Appendix A).

- Severity is an empirical assessment of the consequences of radiation exposure. In RIPD it is a measure of the effects in a typical, *symptomatic* individual. For example, if the incidence at a particular dose is only 50%, severity will reflect the symptoms only seen in half of the population. Five levels of severity are described for each symptom category-- Level 1 being normal and Level 5 indicating the serious effects. The descriptions of each severity level are brief, concise, and comprehensive, making them amenable for use in a performance questionnaire.

In addition to the temporal severity profiles for each symptom, profiles for symptom complexes were also developed (Anno *et al.* 1985). These were formed by combining the temporal profiles of the individual symptoms for each dose range. Symptoms that occur at the same time were grouped as a symptom complex to describe the overarching manifestation of the radiation syndrome at that time. The complexes are identified by a six-digit code number; each digit in that code corresponds to one of the six S/S categories. Although over 15,000 combinations are possible, only 100 symptom complexes pertain to the dose and time ranges of interest here. Of these, 30 to 40 symptom complexes were selected for inclusion in U.S. Army questionnaires designed to obtain personnel judgments of task performance under various degrees of debilitation.

U.S. Army personnel were asked to evaluate the effects of these symptom complexes on performance (Anno *et al.* 1996). The questionnaires framed the questions in terms of the change in time to perform specific tasks with each of the 40 or so symptom complexes. Using time allowed the results to be handled quantitatively. Performance (P) was expressed as the ratio of the time required by a healthy person divided by the time required after radiation exposure.

$$P = t_0/t$$

Since t is always greater than or equal to t_0 , P is always between 0 and 1. The input from all respondents was pooled and the data were analyzed by regression analysis.

Evaluation of the data indicated that UG (nausea and vomiting) and FW were the S/S categories that had the greatest impact on performance. HY and LG distress (diarrhea) occur primarily at supralethal doses and IB (infection and bleeding) was a delayed response (Anno *et al.* 1996). Based on this input, the overall incidence of performance degradation provided by RIPD was defined as the greater of the UG and FW incidence values. This number provides a reasonable indicator of the percentage of an exposed population whose performance will be degraded (Matheson *et al.* 1998).

2.3 Performance Prediction

For all questionnaire respondents, the performance for each task for each S/S complex was determined. The assessments from all respondents were averaged to provide a consensus value for task performance. Using statistical methods and regression analysis (Anno *et al.* 1984, Anno *et al.* 1994), these pooled assessments were used to define the parameters of the logistic function describing the relationship of performance and symptom severity.

Performance is estimated to be:

$$P = \frac{1}{1 + \exp(-\sum_{i=1}^6 \beta_i X_i + C)}$$

where

X_i is the severity level for the i^{th} S/S category

β_i is the i^{th} component of the task-specific regression coefficient vector, and

C is a constant term from the regression analysis.

Although RIPD was designed to predict combat effectiveness in a military context (Anno *et al.* 1984), it is sufficiently versatile to be used in most radiation environments for consequence assessment. One such application, as described in Hu *et al.* 2009, is the prediction of performance consequences in astronauts exposed to radiation from solar particle events.

Section 3.

Description of Physiologically-Based Models

RIPD includes four separate physiologically-based models that are used as primary drivers. The mortality model is based on the MarCell model of the hematopoietic syndrome. Fatigability and weakness predictions are based on a model of lymphocyte kinetics. Prodromal effects of nausea and vomiting are modeled with an upper gastrointestinal (GI) model and gut injury effects are estimated using a lower (GI) model. Each of these models is further described in the following subsections.

3.1 MarCell Model

3.1.1 Model Description

RIPD estimates mortality from hematopoietic syndrome using MarCell (Jones *et al.* 1991), a mathematical model that estimates bone marrow injury following radiation exposure. MarCell was initially developed to predict the hematopoietic response to protracted or fractionated radiation exposures, based on the observed effects with acute doses.

3.1.1.1 Radiation-Induced Cellular Injury

MarCell includes compartments that represent normal, injured, and killed cells. A set of differential equations (see the Appendix of Jones *et al.* 1994) describes the kinetics of cell killing, cell injury, repair of injured cells, death of injured cells, and repopulation of normal cells. Figure 3-1 illustrates flow among the model compartments. With time-dependent radiation dose rate as the input, the model calculates the time-dependent changes in the bone marrow cell populations. MarCell models cellular proliferation, but does not include cell differentiation or senescence.

Cell injury and killing occur with exposure to radiation, thereby reducing the normal cell population. The rates of change of the three cell populations (normal, injured, and killed) are defined as follows:

- rate of change of number of **normal cells** = - (rate of sublethal injury) - (rate of direct killing) + (rate of repair of sublethal injury) + (rate of compensatory repopulation)
- rate of change of number of **injured cells** = - (rate of indirect killing) - (rate of repair of sublethal injury) + (rate of sublethal injury)
- rate of change of number of **killed cells** = (rate of direct killing) + (rate of indirect killing)

The rates of injury and direct killing are determined by the gamma dose rate R_γ , the total dose rate $R_T = R_\gamma + R_{BE_n}R_n$ (where R_n is the neutron dose rate), and the number of normal cells (injury rate = $\lambda_{NI}R_\gamma n_N$ and direct killing rate = $\lambda_{NK}R_T n_N$, respectively). The rate of indirect killing is proportional to the total dose rate and the number of injured cells (indirect killing rate = $\lambda_{IK}R_T n_I$).

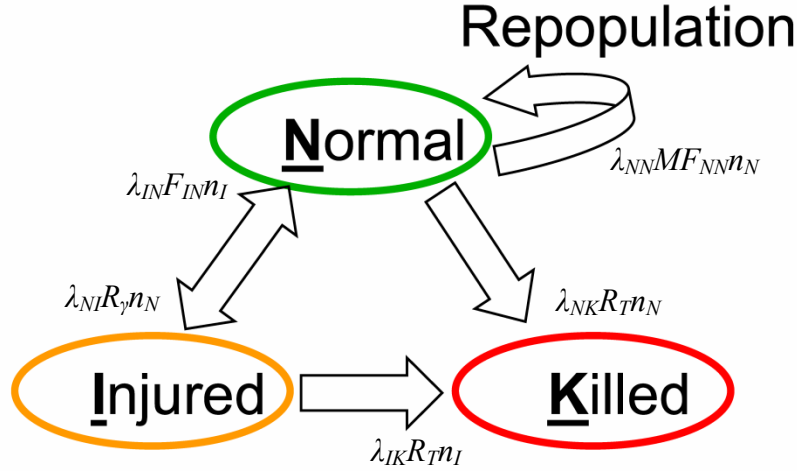


Figure 2. Schematic of MarCell

Parameters are defined in Table 1.

The rates of repair and repopulation are defined similarly, though these terms also include rate-modifying factors that simulate “feedback.” In the absence of this feedback, the rate of repair of sublethal injury is proportional to the number of injured cells; with feedback, the repair rate can vary by a factor of 1 to 2, depending on the surviving fraction of cells s where $s=(n_N+n_I)/n_o$ (thus, *Repair rate* = $\lambda_{NI}(2-s)n_I$). The repopulation rate goes to zero when the surviving fraction approaches 1, and approaches a maximum of twice its normal value when the surviving fraction approaches 0. To account for the mitotic delay after radiation exposure, a multiplicative factor M is also included in the rate of compensatory repopulation: *Repopulation rate* = $\lambda_{NN} M(2-s)(1-s)n_N$. The factor M precludes proliferation when the accumulated dose in gray is greater than the

Table 1. MarCell model components.

Component	Description
n_N	the number of phenotypically normal cells that can undergo mitosis and are at risk of sublethal injury
n_I	the number of cells that can undergo repair of sublethal injury and can be killed by indirect processes
λ_{NI}	rate constant for transition from a normal (N) to an injured (I) state
λ_{IN}	rate constant for repair from an injured (I) to a normal (N) state
λ_{NK}	rate constant for transition from a normal (N) to a killed (K) state
λ_{IK}	rate constant for transition from an injured (I) to a killed (K) state
λ_{NN}	rate constant for repopulation (proliferation) of normal (N) cells
M	mitotic delay factor
F_{NN}	dynamic factor that modifies the effective proliferation rate depending on extent of injury

F_{IN}	dynamic factor that modifies the effective repair rate depending on the extent of injury
R_γ	gamma dose rate (marrow)
R_n	neutron dose rate (marrow)
RBE_n	relative biological effect (neutron dose rate weighting factor)
R_T	$= R_\gamma + RBE_n R_n$, total radiation dose rate (marrow)

time in hours ($M=0$); after the time since initial exposure (hours) has surpassed the accumulated dose (Gy), $M = 1$. Consequently, if the dose rate is less than 1 Gy/h, proliferation is not impaired ($M=1$). If the dose is 2 Gy over the first hour, proliferation resumes 2 hours after initiation of exposure.

In summary, MarCell is defined by the differential equations:

$$\dot{n}_N = -\lambda_{NI}R_\gamma n_N - \lambda_{NK}R_T n_N + \lambda_{IN}F_{IN}n_I + \lambda_{NN}MF_{NN}n_N$$

$$\dot{n}_I = -\lambda_{IK}R_T n_I - \lambda_{IN}F_{IN}n_I + \lambda_{NI}R_\gamma n_N$$

$$\dot{n}_K = \lambda_{NK}R_T n_N + \lambda_{IK}R_T n_I$$

where $R_T = R_\gamma + RBE_n R_n$, R_γ is the gamma dose rate (marrow, Gy/h), and R_n is the neutron dose rate (marrow, Gy/h). RBE_n is the relative biological effectiveness (RBE) for neutron radiation. Because the RBE varies with each organ system, the value varies with each RIPD model component. In MarCell, $RBE_n = 4.25$.

The parameters are defined in Table 3-1. λ_{NI} , λ_{IN} , λ_{NK} , λ_{IK} , and λ_{NN} are maximum likelihood estimates (MLEs) of the rate constants.

$$F_{IN} = 2 - s = 2 - \left(\frac{n_N + n_I}{n_0} \right) \quad \in [1,2]$$

$$F_{NN} = (2 - s)(1 - s) = \left(\frac{n_0 - n_N - n_I}{n_0} \right) F_{IN}$$

The specific cell that constitutes the population critical to hematopoietic lethality is not specified in the MarCell model. Because data were unavailable to identify this critical population, the rate constants could not be experimentally determined. Instead, the rate constants were estimated from animal mortality data.

3.1.1.2 *Probability of Lethality and Calculating the Equivalent Prompt Dose*

The MarCell model assumes that the surviving fraction of at least one population of cells determines the probability of lethality. The minimum surviving fraction (s_{min} , defined below) includes both normal and injured cells. Any radiation exposure that leads to the same surviving fraction is assumed to produce the same lethality (i.e., s_{min} is assumed to be an isoeffect for the probability of lethality). The model further assumes that the dose response curve for mortality with prompt exposures is adequately described by a probit equation. The two defining constants of the probit curve, however, may vary with species, exposure conditions, or other factors. For protracted exposures, anticipated mortality is determined from the lethality of the equivalent prompt dose (EPD) which elicits the same nadir in the surviving cell fraction. This nadir is defined as the minimum cell survival $s_{min}(t)$, where

$$s_{min}(t) = \min_{\tau \in [t_0, t]} (n_N(\tau) + n_I(\tau))$$

and t_0 is the time at which exposure begins. Two exposure scenarios (e.g., two different dose-rate functions) are associated with the same probability of lethality if they lead to the same value of s_{min} . This model assumption (that s_{min} is an isoeffect for the probability of lethality) allows one to use experimental prompt-dose lethality data to predict the lethality of an arbitrary protracted dose. The relationship between cell kinetics and lethality is established with data on acute exposures; the isoeffect allows determinations with protracted and complex exposures.

3.1.1.3 *Fitting the Parameters*

MarCell depends on five parameters that represent cellular kinetics and two parameters that define the relationship between prompt dose and mortality. Coefficients were estimated by maximum-likelihood methods. There were no unique parameter estimates; that is, the likelihood function does not indicate a unique best value and various combinations can produce the same predictions. Without any restrictions, however, it became evident that the family of solutions all had cell kinetics that reflected a cell population that was inconsistent with stem cells or progenitor cells and more consistent with stromal cells. Recent studies have validated this perspective with the finding that bone marrow proliferation is dependent on the viability of osteoblasts in the bone marrow niche. These recent findings are summarized in an ARA technical note (Pellmar 2011).

For determinations of lethality, probit curves for lethality from acute radiation exposure were constructed for a variety of animal models from experimental data (see Jones *et al.* 1996). For humans, RIPD uses the probit for radiation lethality from Anno *et al.* (2003).

3.1.1.4 *Calculating Time to Lethality*

Although MarCell is based on cell populations in the bone marrow, it is useful for evaluation of the probability of lethality regardless of the radiation syndrome (e.g., hematopoietic, gastrointestinal, cardiovascular syndromes) triggering death. Similarly, changes in the same cell population can be used to calculate the projected time to lethality (t_L). In RIPD, estimation of the mean time to death as a function of radiation dose uses the empirical formula

$$t_L = t^* + \frac{a_1}{b_1 + D^\alpha} + \frac{a_2}{b_2 + D^\beta}$$

where

$$t^* = \min\{t | n_N(t) + n_I(t) = s_{min}\} \text{ (hours)}$$

$$a_1 = 878900000, a_2 = 1986600, \alpha = 2.4489, b_1 = 1923000, b_2 = 5821.8, \beta = 1.2$$

and D is the midline tissue equivalent prompt dose (Gy). The time to lethality relationship is based on data both from radiation accidents (Anno *et al.* 1989) and from the atomic bomb detonation at Nagasaki (Levin *et al.* 1992). A regression analysis was used to determine parameter values. The parameter t^* models the time delay in lethality that occurs with protracted exposure to radiation.

3.1.2 Validation and Limitations

MarCell is based on data from a wide range of studies in various species exposed to various radiation qualities at different dose rates. According to the DNA Technical Report from Jones *et al.* (1996), rate constants were estimated from the mortality data in 27 experiments from a total of 18,940 animals with 851 dose response groups. Jones *et al.* (1996) validated the model by predicting the LD₅₀ in 38 rodent studies that were not used for determination of the parameters.

Validation studies used a variety of dose rates (from 0.0008-4.74 Gy/min) and fractionation protocols (from 1.54-7 Gy over hours to 8 weeks). These studies consistently confirmed the ability of the model to predict lethality using the EPD approach (Jones *et al.* 1996). The model was also evaluated with experimental data from non-rodent species under various conditions (e.g., dose rate and RBE). Consequences of human exposures also fit well with model predictions (Jones *et al.* 1994).

MarCell (as originally developed by ORNL) estimates the probability of mortality; it does not predict symptoms or estimate the populations of circulating hematopoietic cells. However, RIPD uses MarCell's EPD and t^* ("time of minimum cell count"; see above) to extend to protracted exposures the IDP prompt exposure symptomatology models that reflect bone marrow damage (e.g., manifest UG distress, IB, HY). The MarCell model only considers proliferation of a single critical cell population and does not consider amplification, differentiation or senescence pathways.

3.2 Fatigability and Weakness Model

Using a model of lymphocyte kinetics, RIPD extends the IDP prompt-dose FW model to protracted radiation exposures. The underlying hypothesis is that lymphocyte damage results in the release of a cytokine that is responsible for the observed FW symptoms (Anno *et al.* 1996). In RIPD's FW model, the lymphopoiesis model of Zukhbaya and Smirnova (1991) is used in

conjunction with a cytokine release/severity response model, parameterized using the IDP prompt exposure FW severity model.

3.2.1 Model Description

After radiation injury FW has a biphasic time course; it has a very early onset (within minutes to hours of radiation exposure) and improves or resolves within a few days but recurs after several days or weeks. In the development of the model, several possible underlying mechanisms were considered because of their time course with very early onsets. The mechanisms included changes in the microvasculature, circulation serotonin levels, and lymphocyte depletion. Lymphocytes were selected because they have a very early response to radiation with a time course similar to FW symptoms, they are a source of many different cytokines, and cytokines were closely linked to FW-type symptoms (Anno *et al.* 1996).

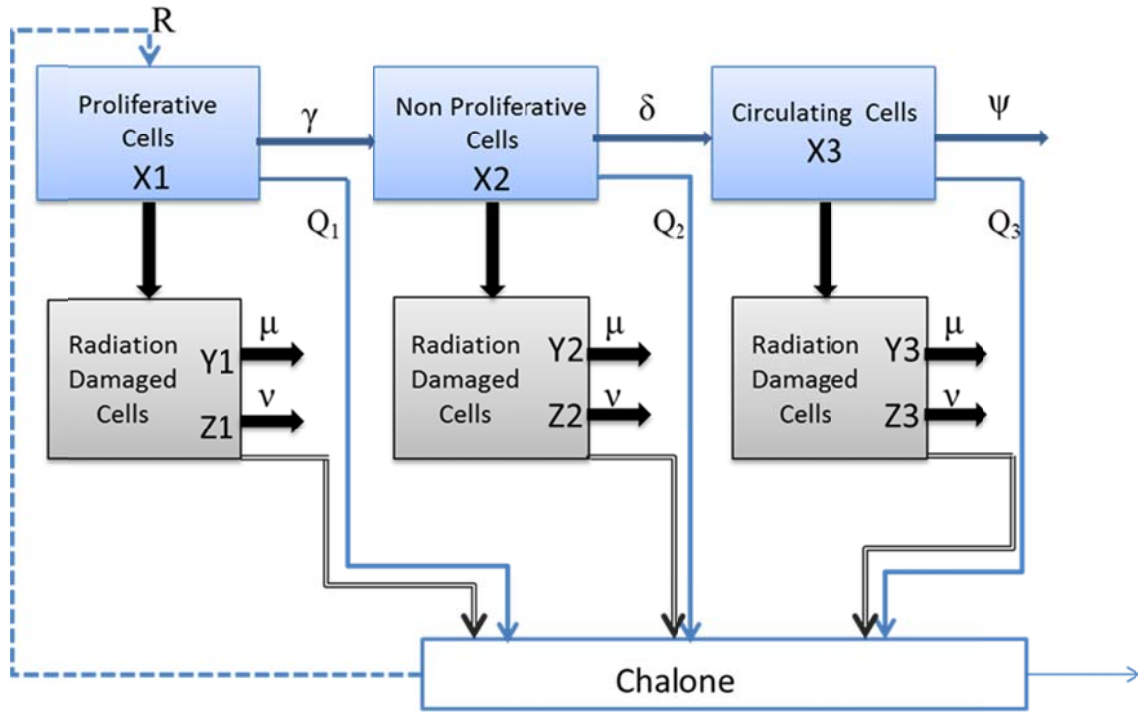


Figure 3. Schematic of lymphopoiesis model.

Parameters are defined in Table 2.

3.2.1.1 Radiation Effects on Lymphocytes

Radiation effects on lymphocytes in the FW model are predicted by the model of Zukhbaya and Smirnova (1991). The model assumes three cellular compartments: the lymphoblast, a dividing progenitor cell (X_1), an intermediate cell type that is not dividing (X_2), and the lymphocytes in

circulation (X_3). A mitotic inhibitor, or chalone, provides feedback that modulates the rate of reproduction of the progenitor cell. The number of cells of each type influences the production of the chalone. The schematic diagram of the lymphopoiesis model is illustrated in Figure 3-2.

With radiation exposure cells can be damaged (Y_i) or heavily damaged (Z_i). The Y and Z cells undergo specific rates of death. The transition from state X to state Y or Z is dependent on radiation dose rate. The transition of cells from compartment X_1 to X_2 occurs at rate γ , from compartment X_2 to X_3 at rate δ , and cells in compartment X_3 undergo natural lymphocyte death at rate ψ . Many parameters in Smirnova's model were estimated from experimental data in the literature. The following equations describe the changes in lymphocytes with radiation exposure:

$$\dot{x}_1 = Rx_1 - \gamma x_1 - \left(\frac{R_T}{D_1}\right)x_1$$

$$\dot{x}_2 = \gamma x_1 - \delta x_2 - \left(\frac{R_T}{D_2}\right)x_2$$

$$\dot{x}_3 = \delta x_2 - \psi x_3 - \left(\frac{R_T}{D_3}\right)x_3$$

$$\dot{y}_k = \left(\frac{R_T}{D_k}\right)\left(\frac{1}{1 + \rho_k}\right)x_k - \mu y_k \quad (k = 1, 2, 3)$$

$$\dot{z}_k = \left(\frac{R_T}{D_k}\right)\left(\frac{\rho_k}{1 + \rho_k}\right)x_k - \nu z_k \quad (k = 1, 2, 3)$$

$$R = \frac{\alpha}{1 + \beta(\sum_{i=1}^3 Q_i(x_i + Uy_i + Vz_i))}$$

where

$$\rho_k = \frac{D_k}{D_{mk} - D_k},$$

$R_T = R_\gamma + RBE_n R_n$, R_γ is the gamma dose rate (midline tissue dose, MLT, Gy/h), and R_n is the neutron dose rate (MLT, Gy/h). For FW, $RBE_n = 1$.

In the absense of radiation exposure (*i.e.*, $R_T = 0$), the nonzero equilibrium point is

$$\bar{x}_1 = \frac{\frac{\alpha}{\gamma} - 1}{\beta \left(Q_1 + Q_2 \left(\frac{\gamma}{\delta} \right) + Q_3 \left(\frac{\gamma}{\psi} \right) \right)}$$

$$\bar{x}_2 = \left(\frac{\gamma}{\delta} \right) \bar{x}_1$$

$$\bar{x}_3 = \left(\frac{\gamma}{\psi} \right) \bar{x}_1$$

which implies
$$\beta = \frac{(\alpha - \gamma)/\psi}{\bar{x}_3 \left(Q_1 + Q_2 \left(\frac{\gamma}{\delta} \right) + Q_3 \left(\frac{\gamma}{\psi} \right) \right)}.$$

Table 2. Parameters for lymphopoiesis model.

Parameter	Description
α	maximum specific reproduction rate of X_1 cells
γ	rate of cell transition from X_1 to X_2 state
δ	rate of cell migration to peripheral circulation
ψ	rate of natural lymphocyte death
μ	rate of death of damaged cells
ν	rate of death of heavily damaged cells
D_k	the traditional 37% survival dose parameter for exponential cell survival in radiobiology; this is the D_0 for X_1 , X_2 and X_3 cells
D_{mk}	the analogous parameter to D_k for lymphocyte interphase death acute dose
$Q_k, Q_k U, Q_k V$	represent relative chalone production for X_k , Y_k , and Z_k cells; $Q_1=1$, $V = (\nu/\mu)U$

3.2.1.2 Cytokine Release

Cytokines were assumed to be released from damaged (Y_2 and Y_3) and heavily damaged cells (Z_2 and Z_3). The time-dependent levels of cytokines were calculated from the rate of release and the rate of deactivation. It was recognized that this may be an oversimplification of the biology but when the model was developed, the data were limited (Anno *et al.* 1996). The endogenous cytokine levels are described by the following equations:

$$\dot{C} = \varepsilon_1 P - \varepsilon_2 C$$

where

$$C(0) = 0$$

$$P = (Y_2 + Y_3 + Z_2 + Z_3)/N_0$$

$$N_0 = \bar{X}_2 + \bar{X}_3$$

ε_1 and ε_2 are cytokine release and deactivation rate constants, respectively.

3.2.1.3 Severity of Fatigability and Weakness

The biphasic nature of the FW response was described by empirically derived equations for early and late response as a function of cytokine concentration and radiation dose. Using the extensive data available for acute doses in radiation therapy patients and nuclear accident victims, an empirical profile of fatigability and weakness was constructed (Anno *et al.* 1996). FW was ranked on a 5-point severity scale. A scale was specifically designed for the modeling because the existing scales designed for individual clinical care were inadequate for modeling (Anno *et al.* 1996). The resulting profile described the time and dose dependence of the severity of FW following acute radiation exposure and was used to fit the cytokine release parameters. The model of radiation effects on lymphocytes in combination with cytokine release allows the extension of the prompt-dose FW data to protracted exposures.

The severity in the early phase of fatigability and weakness is modeled by

$$\tau_1 = \frac{CF^*}{\varepsilon_3} \left(1 - \exp \left(-\ln 2 \left(\frac{C}{\varepsilon_4} \right)^{\varepsilon_5} \right) \right)$$

where

$$F^* = \begin{cases} 1, & F \leq 1 \\ F, & F > 1 \end{cases}$$

$$F = -\log_{10}(\varepsilon_6 N)$$

$$N = \frac{X_2 + X_3}{N_0}$$

and the severity in the later phase of fatigability and weakness is modeled by

$$\tau_2 = \varepsilon_7 \left(1 - \exp \left(-\frac{D + \varepsilon_8}{\varepsilon_9} \right) \right) \cdot \left(\exp \left(-\frac{\varepsilon_{10}}{D} \right) \right) \int_0^t C(s) \cdot F^*(s) ds$$

where ε_i for $i=3$ to 10 are constants and D is the accumulated dose.

The severity of the combined early and late phases of the FW response was defined to be

$$S(t) = 1 + 4 (\tau_1 + \tau_2)$$

if $1 + 4 (\tau_1 + \tau_2) \in [1,5]$.²

3.2.1.4 Parameter Estimation

In the lymphopoiesis component of the model, the values of many of the constants were derived from experimental data (Zukhbaya and Smirnova 1991). Values of α , γ , δ , and ψ were based on normal lymphocytes, in the absence of radiation. Values of D_k , D_{mk} , μ , and ν were derived directly from radiobiology experiments. Q_1 was set to 1. Q_2 , Q_3 , and U were determined by best fits of the model to experimental data for the dynamic changes in lymphopoiesis after perturbation of the system. The values of ε_i (for $i=1$ to 10) in the cytokine release and FW response models were calculated to best fit the empirical data for fatigability and weakness (severity response profiles for acute exposures). The constants for hematopoiesis (α , γ , δ , ψ , μ , and ν) were also allowed to change from the initial estimates based on data. In this process, many of the rates increased; most notable was the increase in the death rate of the damaged cells. The changes suggested that, for this purpose, the reproductive rate of X_1 cells was maximized. The biology behind this finding was not known but it was suggested that this model may be using lymphopoiesis to represent other contributions of the immune system.

3.2.2 Validation and Limitations

The lymphopoiesis model is well documented in Zukhbaya and Smirnova (1991) and in Smirnova (2010). Original parameters were determined for both rodents and humans from experimental and clinical studies. The model was found to simulate the cellular changes after both acute and protracted exposures to ionizing radiation.

Anno *et al.* (1996) summarize the clinical and accident studies that were used to create the severity profiles used in the FW model. Reports of fatigability were often subjective, though some studies measured surrogate endpoints such as capacity for exercise. Many of the studies did not clearly link symptom severity to dose. However, taken as a whole, the studies provided information on the time of onset and recovery and suggested a biphasic behavior within a certain range of doses.

The FW model seems to provide a realistic projection of the symptoms following a variety of radiation exposures. However, there are some dose rate effects that may not be fully accounted for. The model was not recommended for dose rates less than 0.074 Gy/h.

Some of the biological assumptions upon which the FW model is based are inconsistent with the most recent experimental data. The current literature suggests that rather than cytokines being released from damaged lymphocytes to produce FW, cytokines are released from T cells that persist after acute exposures. Specific cytokines have been linked with fatigability and weakness following radiation therapy and other disorders (*e.g.*, Bower *et al.* 2009, Wang *et al.* 2010) though with some conflicting findings (*e.g.*, Geinitz *et al.* 2001, Ahlberg *et al.* 2004). Recent

² $S(t) = 1$ if $1 + 4 (\tau_1 + \tau_2) < 1$, $S(t) = 5$ if $1 + 4 (\tau_1 + \tau_2) > 5$.

studies show a likely association between increased T-cell lymphocytes (especially CD4+ and CD56+ T cells) and fatigue (*e.g.*, Bower *et al.* 2003, Lorusso *et al.* 2009). Consistent with a role for these cells in radiation-induced fatigability is the observation that radiation exposure can increase some T-cell populations (*e.g.*, Nagayama *et al.* 2002, Qu *et al.* 2010).

3.3 Upper GI Model

A model of the emetic pathway enables RIPD to extend the IDP prompt-dose model of prodromal UG distress to protracted radiation exposures. RIPD's UG model is based on the hypothesis that radiation causes the release of a neuroactive substance that is responsible for the observed UG distress symptoms.

3.3.1 Model Description

3.3.1.1 Emetic Pathway

The UG distress model assumes that radiation acts on a pool of enterochromaffin cells (ECs) in the gut that synthesize and store a neuroactive substance (NAS, *e.g.*, serotonin (5HT)) that initiates the emetic response. The reservoir of NAS, C , is assumed to be depleted by the release of the NAS after radiation exposure. The depletion depends on dose sensitivity (D_0) and dose rate (R_T): $(R_T/D_0) * C$. The contents of C are replenished with a rate constant of μ : $\mu * (C_0 - C)$. The underlying process has not been linked to any known mechanisms but fits with experimental and clinical observations (see Anno *et al.* 1991, Anno *et al.* 1996). These features allow for the decreasing effectiveness of successive radiation doses (*i.e.*, habituation to the radiation exposure). Figure 3-3 illustrates the compartments in the model of the emetic response.

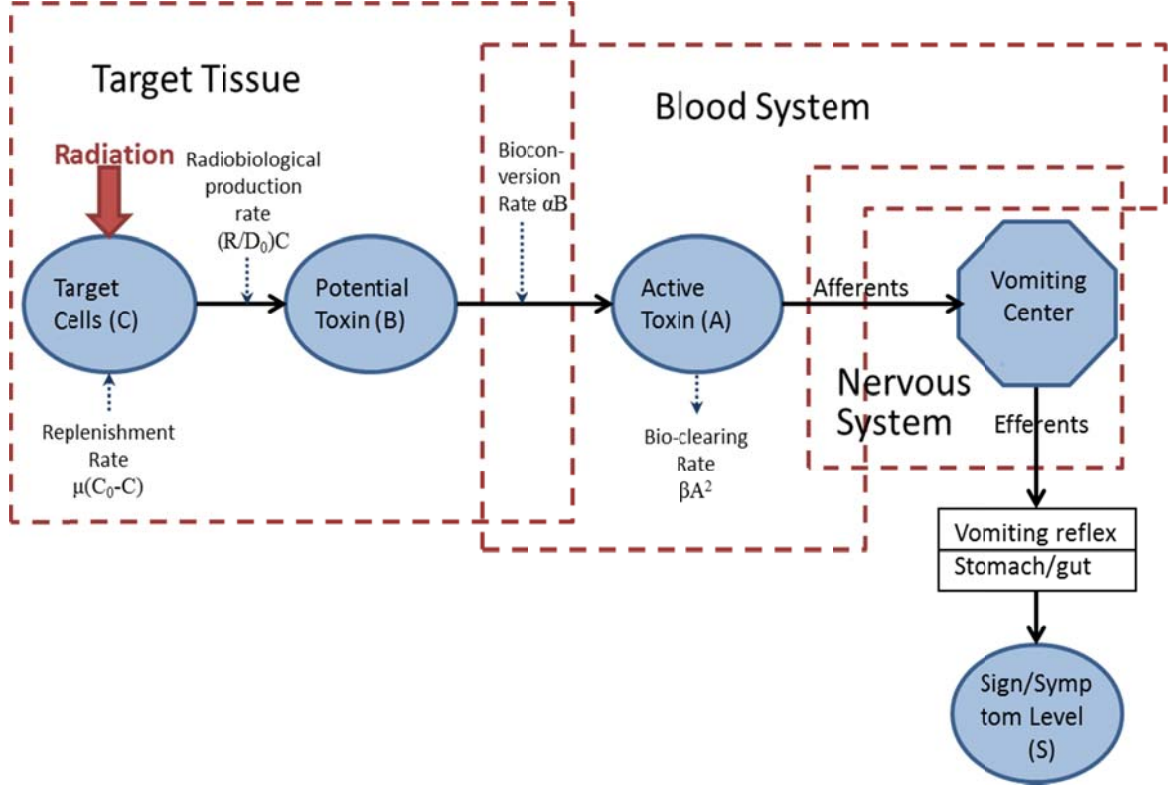


Figure 4. Schematic of emetic response in UG distress model.
Parameters are defined in Table 3.

In the model, radiation exposure transforms the reservoir of the NAS (C) to a “potential toxin”, B . The shift from C to B may be considered the transfer of the NAS to a vesicle pool ready for exocytosis. B is released as the “active toxin,” A . The active toxin A activates the emetic centers in the brain through vagal afferents and the circulatory system. This step encompasses the processes of release, transport, and activation of the central vomiting centers. The potential toxin B is converted to A at a rate of α . The active toxin A is cleared at a rate of β which simulates the degradation of the NAS. These first three steps, represented by the equations for \dot{C} , \dot{B} , and \dot{A} , simulate the emetic mechanistic pathways. The equations for B and A were adjusted to fit the empirical data by adding scaled dose factors to the α and β rate constants ($(1+q^2)(\ln P)^{1/3}$ and Q , respectively). Levels of C , B , and A are expressed in terms of radiation dose units (Gy). This abstraction is used since no actual quantities can be determined. The emetic pathway model is given by

$$\dot{C} = -\left(\frac{R_T}{D_0}\right)C + \mu(C_0 - C)$$

$$\dot{B} = \left(\frac{R_T}{D_0}\right)C - \alpha(1 + q^2)(\ln P)^{1/3}B$$

$$\dot{A} = \alpha(1 + q^2)(\ln P)^{1/3}B - \beta QA^2$$

where

$$P = \begin{cases} \frac{\eta q}{B}, & \frac{\eta q}{B} > 1, B > 0 \\ 1.1, & \frac{\eta q}{B} \leq 1, B > 0 \end{cases}$$

$$Q = \begin{cases} \frac{1}{q} + q, & D_T > 0 \\ 0, & D_T = 0 \end{cases}$$

$$q = (D_T/b)^{3/4}$$

$$D_T = \begin{cases} \int_{t_0}^t R_T(s)ds, & t \geq t_0 \\ 0, & t < t_0 \end{cases}$$

As in other modules, $R_T = R_\gamma + RBE_n R_n$ where R_γ is the gamma dose rate (MLT, Gy/h) and R_n is the neutron dose rate (MLT, Gy/h). $RBE_n = 1$ in RIPD's UG model.

3.3.3.2 Severity of Prodromal Emetic Response

Time-dose response profiles for acute exposures were constructed from empirical data from accidents and patient populations (Anno *et al.* 1985). Severity of UG distress (S) is described by a five level severity scale.

The response of the emetic centers elicits the signs and symptoms of UG distress. The levels of A are converted to a measure of severity of emesis S . The relationship between S and A was based on the time-dose response profiles. It is assumed that the severity was half maximal when A was half maximal. The shape parameter γ determines the steepness of the severity response. The function used introduces a threshold-type behavior.

$$S = 1 + 4 \left(1 - \exp \left(-\ln 2 * \left(\frac{A}{A_{0.5}} \right)^\gamma \right) \right)$$

Using the calculated levels of A , prediction of nausea and vomiting with protracted exposures is possible.

3.3.3.3 Parameter Estimation

The nine parameters of the equations were optimized for the best fit of the empirical data. They are not known to have any direct biological correlates. The parameters are listed in Table 3-3.

Table 3. Parameters for UG model

Parameter	Description
α	Neuroactive agent release coefficient
β	Neuroactive agent metabolism/clearing coefficient
μ	Neuroactive agent generation rate
C_0	Initial neuroactive agent level in compartment C (synthesis and storage pool)
D_0	Characteristic target tissue dose
$A_{0.5}$	Half maximum value of A (released neuroactive agent) for severity response function (S)
γ	Slope constant of S response function
η	Modeling constant
b	Modeling constant

3.3.2 Validation and Limitations

This model is largely based on the effects of prompt radiation doses on the symptoms of nausea and vomiting. Anno *et al.* (1991) and Anno *et al.* 1996 review the data available on emetic mechanisms at the time the model was constructed. A comprehensive review of accident victims and radiation therapy patients also provided data for the dose- and time- dependent profiles (*e.g.*, Anno *et al.* 1985, Anno *et al.* 1989).

Because the ferret's emetic response to radiation is similar to the human response, this animal model could be used to test the ability of the UG model to predict the emetic response to protracted and fractionated doses. From data for acute doses (King 1988), severity curves were constructed for the ferret. Model parameters were fit to the curves for the acute response. The model was used to make predictions for fractionated exposures. The experimentally determined emetic response in ferrets exposed to 3 fractions of 2 Gy over 4 hours reasonably agreed with the predicted outcomes (McClellan *et al.* 1992).

The emetic pathway model's mechanistic underpinnings are not as solid as those of the above lymphopoiesis model. It is consistent with the extensive research on emetic mechanisms but does not attempt to model the many and complex pathways contributing to the behavior. The compartments are theoretical and their interrelationships are defined by parameters developed to fit the empirical data. However, it has been effective in predicting the impact of complex patterns of radiation exposure and consequently useful in a model of radiation-induced performance decrement. Little new experimental data has been collected since the creation of the model to fill in the knowledge gaps that would allow improvements to the mechanistic basis.

At the time of model development, it was generally accepted that nausea is a mild manifestation of the same mechanisms as emesis. Recent evidence, however, suggests that it may be independent anatomically and pharmacologically (see Andrews and Horn 2006). Modeling of nausea, therefore, may need an alternative approach. However, data are even more limited for this endpoint than for emesis because of the difficulties of studying it in an animal model and of standardizing and quantifying it in man.

3.4 Gut Injury Model

RIPD uses a model of cell loss in the intestinal epithelium to extend the IDP model of prompt-dose LG distress to protracted radiation exposures. This Gut Injury Model (GIM) in RIPD uses nested components: the lethal/potentially-lethal (LPL) model of Curtis (1986) estimates cell survival with radiation, the proliferation and intracellular repair (PAIR) model combines the LPL equations with equations for cell proliferation and mitotic delay, and a compartmental model of the cells of the intestinal epithelia is built on PAIR to calculate epithelial cell loss in the gut. The compartmental model considers the proliferating cells of the crypts (clonogenic cells), which develop into transit cells, which, in turn, move out of the crypt to become the mature cells of the villi. The cell loss is used to estimate severity of radiation-induced diarrhea.

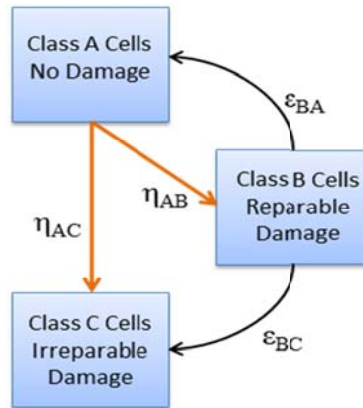


Figure 5. Schematic of the LPL component of the GIM.
Parameters are defined in Table 4.

Table 4. Variables and parameters for the GIM.

Component	Description
N_A	Number of proliferating cells with no lesions (uninjured cells)
N_B	Number of proliferating cells with one or more PL lesions but no lethal lesions (injured cells)
N_C	Number of proliferating cells with at least one lethal lesion (mitotically dead cells)
N_T	Number of cells in the transit compartment
N_V	Number of cells in the villus compartment
n_B	Mean number of PL lesions in Class B cells
n_C	Mean number of L lesions in Class C cells
n_{PL}	Mean number of PL lesions in a hypothetical pool of cells with a Poisson

	distribution of PL lesions and for which the number of cells with one or more PL lesions and no lethal lesion is N_B
H	Homeostasis factor
M	Mitotic delay factor
Q	Cellular damage
A	Threshold at which repair of cellular damage is saturated
λ	Instantaneous clonogen division rate
λ_m	Maximum cell division rate
γ	Normal division rate which balances normal attrition
δ	Acute dose mitotic delay constant
θ	Rate of transition of crypt cells (clonogenic compartment) to transit cells
η_{AB}	Rate of production of potentially lethal lesions
η_{AC}	Rate of production of lethal lesions
ϵ_{BA}	Rate of repair of potentially lethal lesions
ϵ_{BC}	Rate of fixation of lethal lesions
ϕ_N	Flux of cells – clonogen to transit, equals $\theta \cdot N$
ϕ_T	Flux of cells – transit to villus
ϕ_V	Flux of cells – villus attrition
a	Factor to moderate the increase in mitotic rate as N_T decreases

3.4.1 Model Description

The GIM assumes that lower gastrointestinal (GI) distress is associated with cell loss in the intestinal epithelium. Lethality from GI effects occurs within about 5-7 days. Diarrhea occurs at a lower radiation dose than lethality and has an onset of 3-5 days. The diarrhea occurring within the first day of exposure is not considered. The 5-day time course is consistent with the time to minimum cell population of the intestinal epithelium with acute, high radiation doses. The loss of villi is thought to prevent mucosal absorption of fluid, resulting in hypovolemic shock causing “gut death.”

3.4.1.1 Radiation Effects on Cells of the Gut

The LPL model considers two types of lesions: lethal (L) and potentially-lethal (PL). A Poisson distribution is assumed for each type of lesion since they are produced at random by radiation exposure. The L lesions, with an average number equal to n_C per cell, cannot be repaired and prevent mitosis. PL lesions, with a mean equal to n_B per cell, can be repaired by a process with linear kinetics. Given enough time, all PL lesions would be repaired to healthy cells or misrepaired to generate L lesions.

Cells are sorted into three classes: N_A (Class A cells, uninjured cells); N_B cells (Class B cells, injured cells) with one or more PL lesions but no L lesions; and N_C cells (Class C cells, mitotically dead cells) with at least one L lesion. Class A cells proliferate, but Class C cells do not. Although mitotically dead, Class C cells remain in the tissue and are assumed to differentiate into functional cells and to influence homeostasis. The schematic of the LPL model is shown in Figure 3-4.

To adapt the LPL model to proliferating tissue, the PAIR model takes into account the statistical distribution of the lesions among the cells and the impact of mitotic reproduction and mitotic death on that distribution. The distribution of lesions in the Class B cells is assumed to be a truncated Poisson distribution in this hypothetical pool, allowing proliferation of Class A cells without influencing this statistical distribution. The equations describing the distribution of cells take into consideration the direct effect of radiation exposure, mitotic death, proliferation, repair of injured cells, misrepair, and mitotic delay.

The rate equations for the Class A, B, and C cells are:

$$\dot{N}_A = \lambda N_A - (\eta_{AB}R_Y + \eta_{AC}R_T)N_A + \epsilon_{BA}(n_B - n_{PL})N_B - \theta N_A$$

where λN_A describes the proliferation of A cells

$(\eta_{AB}R_Y + \eta_{AC}R_T)N_A$ is the loss of Class A cells due to radiation injury

$\epsilon_{BA}(n_B - n_{PL})N_B$ is the repair of injured cells (Class B cells)

θN_A is the transition of “clonogenic compartment” cells to the “transit compartment”

$$\dot{N}_B = \lambda N_B + \eta_{AB}R_Y N_A - \eta_{AC}R_T N_B - \epsilon_{BA}(n_B - n_{PL})N_B - \epsilon_{BC}n_{PL}n_B N_B - \theta N_B$$

where λN_B describes the proliferation of Class B cells³

$\eta_{AB}R_Y N_A$ is the influx of radiation injured Class A cells

$\eta_{AC}R_T N_B$ is the radiation injury of Class B cells (to become Class C cells)

$\epsilon_{BA}(n_B - n_{PL})N_B$ is the repair of injured cells (Class B cells) to become Class A cells

$\epsilon_{BC}n_{PL}n_B N_B$ is the misrepair of Class B cells (to become Class C cells)

θN_B is the transition of “clonogenic compartment” cells to the “transit compartment”

$$\dot{N}_C = \lambda_C N_C + \eta_{AC}R_T(N_A + N_B) + \epsilon_{BC}n_{PL}n_B N_B - \theta N_C$$

where $\lambda_C N_C$ describes the proliferation of Class C cells

λ_C is zero except at extremely low total radiation dose and limited radiation injury
 $(n_C \cdot D_T < 0.118 \text{ Gy where } n_C = \lambda_C)$ when it equals λ

³ The description provided in the current document describes the system as mathematically implemented in RIPD. These equations, however, are not consistent with report TR157 (Anno *et al.*, 1991). In that document, Class B and C cells do not proliferate. If a Class B cell with at least one unrepaired PL lesion enters mitosis, the cell fails to divide and is reproductively dead. Proliferation in Class B cells moves them to Class C.

$\eta_{AC}R_T(N_A + N_B)$ is the lethal effect of radiation on Class A and B cells

$\epsilon_{BC}n_{PL}n_BN_B$ is the misrepair of Class B cells (to become Class C cells)

θN_C is the transition of “clonogenic compartment” cells to the “transit compartment”

The mean number of PL lesions in Class B cells is affected by radiation exposure, mitosis of Class A cells, repair and misrepair of PL lesions. The rate equation for n_{PL} is

$$\dot{n}_{PL} = \eta_{AB}R_YJ\left(\frac{n_{PL}}{n_B}\right)\left(\frac{1}{1-(n_B-n_{PL})}\right) - \epsilon_{BC}n_{PL}n_B(2-(n_B-n_{PL}))\left(\frac{n_{PL}}{n_B}\right)\left(\frac{1}{1-(n_B-n_{PL})}\right) - \epsilon_{BA}n_{PL}$$

where

$\eta_{AB}R_YJ\left(\frac{n_{PL}}{n_B}\right)\left(\frac{1}{1-(n_B-n_{PL})}\right)$ describes the changes due to mitosis and radiation exposure,

$\epsilon_{BC}n_{PL}n_B(2-(n_B-n_{PL}))\left(\frac{n_{PL}}{n_B}\right)\left(\frac{1}{1-(n_B-n_{PL})}\right)$ is the effect of misrepair of PL lesions,

$\epsilon_{BA}n_{PL}$ is the effect of repair of PL lesions,

and

$$n_B = \frac{n_{PL}}{1 - e^{-n_{PL}}}$$

$$J = \begin{cases} 1 - (n_B - 1)\left(\frac{N_A}{N_B}\right), & R_Y > 0, N_B > 0 \\ 1, & R_Y > 0, N_B = 0, n_B \neq 1 \\ 0, & R_Y > 0, N_B = 0, n_B = 1 \text{ or } R_Y = 0. \end{cases}$$

3.4.1.2 Compartmental Model of the Gut Epithelia

The GIM applies PAIR to the hierarchical structure of the intestinal epithelium. The PAIR model calculates the number of clonogenic cells. The GIM uses this input to track the number of cells in three linked compartments: the clonogens in the crypts, the transit cells in the crypts, and the functional cells of the villi. Figure 3-5 illustrates the schematic for the cellular compartments in the gut.

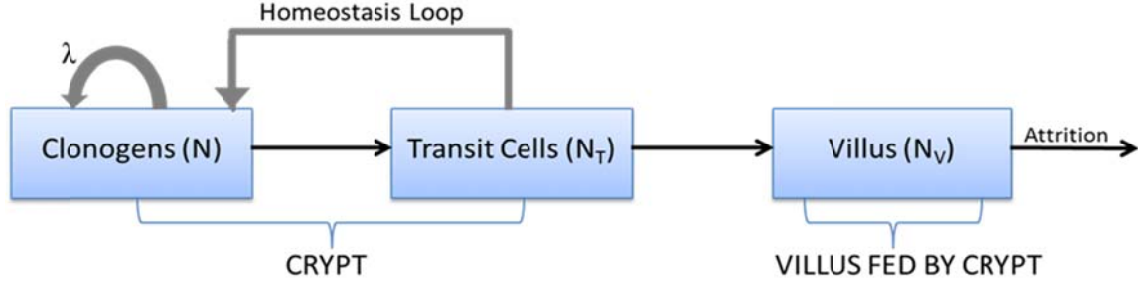


Figure 6. Schematic of the cellular components in the GIM.

The rate equations for N_T and N_V are:

$$\dot{N}_T = \phi_N - \phi_T \quad \text{where } \phi_N = \theta \cdot N$$

$$\dot{N}_V = \phi_T - \phi_V$$

$$\theta = g\left(\frac{N}{N_0}\right) M \gamma,$$

where M is the mitotic delay factor and γ is the normal division rate (see below)

$$g(u) = \begin{cases} 1, & 0 \leq u < 1 \\ u, & u \geq 1 \end{cases}$$

$$\phi_T = \begin{cases} h\left(\frac{N_V}{N_{V0}}\right) \gamma N_0, & 0 < N_T < N_{T0} \\ \min\left\{h\left(\frac{N_V}{N_{V0}}\right) \gamma N_0, \phi_N\right\}, & N_T = 0 \\ \max\left\{h\left(\frac{N_V}{N_{V0}}\right) \gamma N_0, \phi_N\right\}, & N_T = N_{T0} \end{cases}$$

$$h(u) = \begin{cases} 2 - u, & 0 \leq u \leq 1 \\ 1, & u \geq 1 \end{cases}$$

$$\phi_V = \begin{cases} \gamma N_0, & 0 < N_V < N_{V0} \\ \min\{\gamma N_0, \phi_T\}, & N_V = 0 \\ \max\{\gamma N_0, \phi_T\}, & N_V = N_{V0} \end{cases}$$

$$N = N_A + N_B + N_C$$

At equilibrium (N_0 = initial number of Class A cells), the number of transit cells is assumed to be two thirds of the total crypt cells ($N_T = 2*N_0$). Experimental data suggest that the number of functional cells of the villi (N_V) can range between 1.7 to 6.7 times N_0 . Only the clonogenic cells are treated as radiation sensitive because of their high rate of proliferation. A tissue dose of 15 Gy will kill nearly all clonogens, resulting in denudation of the villi in about 6-7 days in man. The rate of cell division (λ) depends on a homeostatic factor (H) and a mitotic delay factor (M) modifying the normal division rate which balances normal attrition (γ).

$$\lambda = HM\gamma$$

Homeostatic equilibrium is assumed to be maintained by some communication among compartments. The model modifies the rate of cell division (compensatory proliferation) with H based on N_T because of proximity. H is maximal when $N_T=0$. Transit cells are not allowed to exceed the equilibrium value and the growth of the clonogenic compartment is limited to twice its normal size (using the function $f(u)$). To account for the delay in rapid proliferation despite cell depletion, the exponent “a” was introduced, moderating the increase in cell division rate as N_T decreases.

$$H = 1 + \left(\frac{\lambda_m - \gamma}{\gamma} \right) \left(1 - \left(\frac{N_T}{N_{T0}} \right)^a \right) f\left(\frac{N}{N_0}\right)$$

$$f(u) = \begin{cases} 1, & 0 \leq u \leq 1 \\ 2 - u, & 1 \leq u \leq 2 \\ 0, & u \geq 2 \end{cases}$$

The rate of cell division also depends on M due to the slowing of the rate of cell division by radiation exposure. M is modeled on the concept of a saturable repair enzyme where activation of the enzyme reduces the rate of cell cycling.

Damage (Q) is reduced by the actions of the finite pool of repair enzymes. Repair is saturated at a threshold of A .

$$M = 1 - \frac{Q}{A + Q}$$

$$\dot{Q} = R_\gamma - \frac{\lambda_m}{\delta} \left(\frac{Q}{A + Q} \right)$$

As in other modules, $R_T = R_\gamma + RBE_n R_n$ where R_γ is the gamma dose rate (MLT, Gy/h) and R_n is the neutron dose rate (MLT, Gy/h). $RBE_n = 7$ in GIM.

3.4.1.3 *Severity of Lower Gastrointestinal Distress*

The severity of lower gastrointestinal distress is estimated to be

$$S = 1 + 4 \exp \left(-\ln 2 * \left(\frac{\tan \left(\frac{\pi}{2} \frac{N_V}{N_{Vo}} \right)}{\chi} \right)^{\xi_v} \right)$$

where χ and ξ_v were chosen based on prompt dose severity response data.

3.4.1.4 Parameter Estimation

The LPL model reflects the basic radiobiological response of cell populations in general. The LPL model links directly to the parameters that are used to define cell survival curves. Consequently, many of the parameters of the GIM were derived from experimental data, primarily from rodent cells. Where appropriate, values were adjusted for the human response. Parameters defining the cell numbers in the compartments at equilibrium and the cell loss by attrition from the villi were selected to fit physiological data and to reproduce the time course of gut denudation after acute radiation.

3.4.2 Validation and Limitations

The GIM was based on extensive data from rodent models (reviewed by Anno *et al.* 1991). Observations of GI death and villi cell populations with acute and protracted doses were used to test the model. Fluid loss in rodents was also compared to villi populations. The model predictions showed good correlations with experimental data. Parameters were adjusted for the characteristics of human gut and its response to radiation. Human symptomatology is based on the prodromal effects of radiation described in Anno *et al.* (1989) and Baum *et al.* (1984).

The GIM provides a mechanistic description of radiation injury to the intestine. From an analysis of epithelial cell loss in the intestine, it provides a good representation of the severity of lower GI distress for acute and protracted doses. However, the model does not consider the vascular changes in the gut that result within a few days of radiation exposures of 5-10 Gy, nor does it consider the functional changes that have been observed with sub-lethal radiation doses. Furthermore, the model does not take into consideration the effects of radiation on functional properties of gut epithelium and it does not consider the changes that occur in gastric motility that could contribute to diarrhea (see MacNaughton 2000). As efforts move forward to model combined injury, a major drawback of GIM is the absence of humoral inputs that might modulate gut injury or secretion of messengers that might impact other organs (*e.g.*, Kiang *et al.* 2010). Recent efforts have demonstrated a correlation of decreased citrulline in the circulation with radiation-induced damage to the gut (Lutgens *et al.* 2003). The level of citrulline is thought to reflect the volume of gut epithelium and, consequently, the available clinical data would provide an approach for validation of the model's predictions in man.

Section 4.

Summary and Conclusions

RIPD combines physiologically-based and empirical models to predict performance decrement and lethality following exposure to ionizing radiation. The model is sufficiently versatile to assess anticipated functional incapacitation after exposures to prompt, protracted, and complex exposure histories. RIPD takes into consideration both the gamma and the neutron exposures that would be expected after a nuclear detonation. It has proven to be an excellent tool with applications for military as well as space missions.

RIPD was designed for the specific tasks of military personnel in the past decades and may require updates to reflect the changing functions of soldiers and airmen in the 21st century to include such tasks as operating complex equipment or computer programs. While the current version of RIPD has several physiologically-based components, it depends heavily on empirical relationships. Some of the physiological components would benefit from an update to reflect recent advances in scientific knowledge. Advances in our understanding of the pathophysiology of radiation injury may allow the biology to be reflected with greater fidelity in the mathematical model. Today's radiation exposure scenarios require assessment of health risks in addition to performance decrement. Improvements to existing physiological components and addition of new component models will allow the program to address this need. Furthermore, new physiologically-based components will facilitate the integration of treatments and of other injuries (such as burns, wounds, and infection) that are likely to be encountered after a nuclear event, resulting in a model of combined injury.

RIPD has been, and continues to be, the primary DoD model for prediction of functional impairment after radiation exposures. While there are several components of the model that would benefit from updates, it remains a valid tool for this purpose. RIPD will serve as a good platform for expansion into new models of health effects and combined injury. With these enhancements, RIPD can evolve into a casualty prediction model that will help military and medical planners predict the incidence of performance incapacitation and health effects, allowing more accurate estimations of time-phased casualties, patient streams, and medical care requirements.

Section 5.

References

- Ahlberg, K., Ekman T., and Gaston-Johansson F., 2004. "Levels of Fatigue Compared to Levels of Cytokines and Hemoglobin during Pelvic Radiotherapy: a Pilot Study," *Biol Res Nurs* 5(3):203–210.
- Andrews, P.L.R., and Horn C.C., 2006. "Signals for nausea and emesis: Implications for models of upper gastrointestinal diseases," *Auton Neurosci*, 125(1-2):100–115.
- Anno, G. H., Dore M.A., Roth J.T., LaVine N.D., and Deverill A.P., 1994. *Predicted Performance of Infantry and Artillery Personnel Following Acute Radiation or Chemical Agent Exposure*. DNA-TR-93-174, Defense Nuclear Agency, Alexandria, VA.
- Anno, G.H., Baum S.J., Withers H.R., and Young R.W., 1989. "Symptomatology of acute radiation effects in humans after exposure to doses of 0.5-30 Gy," *Health Phys*, 56(6):821–838.
- Anno, G.H., McClellan G.E., and Dore M.A., 1996. *Protracted Radiation-Induced Performance Decrement Vol 1 - Model Development*. DNA-TR-95-117-V1, Defense Nuclear Agency, Alexandria, VA.
- Anno, G. H., Wilson D.B., and Baum S.J., 1985. *Severity Levels and Symptom Complexes for Acute Radiation Sickness: Description and Quantification*. DNA-TR-86-94, Defense Nuclear Agency, Alexandria, VA.
- Anno, G. H., Wilson D.B., and Dore M.A., 1984. *Nuclear Weapons Effect Research at PSR, 1983: Acute Radiation Effects on Individual Crewmember Performance*. DNA-TR-85-52. Defense Nuclear Agency, Alexandria, VA.
- Anno, G.H., McClellan G.E., Dore M.A., and Baum S.J., 1991. *Biological Effects of Protracted Exposure to Ionizing Radiation: Review, Analysis, and Model Development*. DNA-TR-90-157, Defense Nuclear Agency, Alexandria, VA.
- Anno, G.H., Young R.W., Bloom R.M., and Mercier J.R., 2003. "Dose response relationships for acute ionizing-radiation lethality," *Health Phys*, 84(5):565–575.
- Baum, S.J., Anno G.H., Young R.W., and Withers H.R., 1984. *NUCLEAR WEAPON EFFECT RESEARCH AT PSR -Symptomatology of Acute Radiation Effects in Humans after Exposure to Doses of 75 to 4500 Rads (cGy) Free-In-Air*. DNA-TR-85-50, Defense Nuclear Agency, Alexandria, VA.
- Bower, J.E., Ganz P.A., Aziz N., Fahey J.L., and Cole S.W., 2003. "T-Cell Homeostasis in Breast Cancer Survivors With Persistent Fatigue," *JNCI Journal of the National Cancer Institute*, 95(15):1165–1168.

- Bower, J.E., Ganz P.A., Tao M.L., Hu W., Belin T.R., Sepah S., Cole S., and Aziz N., 2009. "Inflammatory biomarkers and fatigue during radiation therapy for breast and prostate cancer," *Clin. Cancer Res.* 15(17):5534-5540.
- Curtis, S.B., 1986. "Lethal and potentially lethal lesions induced by radiation--a unified repair model," *Radiat. Res.* 106(2):252-270.
- Geinitz, H., Zimmermann F.B., Stoll P., Thamm R., Kaffenberger W., Ansorg K., Keller M., Busch R., van Beuningen D., and Molls M., 2001. "Fatigue, serum cytokine levels, and blood cell counts during radiotherapy of patients with breast cancer," *Int. J. Radiat. Oncol. Biol. Phys.* 51(3):691-698.
- Hu, S., Kim M-H.Y., McClellan G.E., and Cucinotta F.A., 2009. "Modeling the acute health effects of astronauts from exposure to large solar particle events," *Health Phys.* 96(4):465-476.
- Jones T.D., Morris M.D., and Hasan J.S., 1996. *Environmental Risk Assessments Based on Bone Marrow Cell Kinetic*. DNA-TR-94-99, Defense Nuclear Agency, Alexandria, VA.
- Jones T.D., Morris M.D., and Young R.W., 1991. "A mathematical model for radiation-induced myelopoiesis," *Radiat. Res.* 128(3):258-266.
- Jones T.D., Morris M.D., and Young R.W., 1994. "Dose-rate RBE factors for photons: hematopoietic syndrome in humans vs stromal cell cytopenia," *Health Physics*, 67(5):495-508.
- Kiang J.G., Jiao W., Cary L.H., Mog S.R., Elliott T.B., Pellmar T.C., and Ledney G.D., 2010. "Wound trauma increases radiation-induced mortality by activation of iNOS pathway and elevation of cytokine concentrations and bacterial infection," *Radiat. Res.* 173(3):319-332.
- King G.L., 1988. "Characterization of radiation-induced emesis in the ferret," *Radiat. Res.* 114(3):599-612.
- Levin S.G., Young R.W., and Stohler R.L., 1992. "Estimation of median human lethal radiation dose computed from data on occupants of reinforced concrete structures in Nagasaki, Japan," *Health Phys.* 63(5):522-531.
- Lorusso L, Mikhaylova S.V., Capelli E., Ferrari D., Ngonga G.K., and Ricevuti G., 2009. "Immunological aspects of chronic fatigue syndrome," *Autoimmun Rev*, 8(4):287-291.
- Lutgens L.C.H.W., Deutz N.E.P., Gueulette J., Cleutjens J.P.M., Berger M.P.F., Wouters B.G., von Meyenfeldt M.F., and Lambin P., 2003. "Citrulline: a physiologic marker enabling quantitation and monitoring of epithelial radiation-induced small bowel damage," *Int. J. Radiat. Oncol. Biol. Phys.* 57(4):1067-1074.

- MacNaughton W.K., 2000. "Review article: new insights into the pathogenesis of radiation-induced intestinal dysfunction," *Aliment. Pharmacol. Ther.*, 14(5):523–528.
- Matheson L.N., Dore M.A., Anno G.H., and McClellan G.E., 1998. *Radiation-Induced Performance Decrement (RIPD). User's Manual. Version 2.0*. DNA-TR-95-91. Defense Nuclear Agency, Alexandria, VA.
- McClellan G.E., Anno G.H., King G.L., and Young R.W., 1992. "Evaluation of predictive algorithm for the human emetic response to protracted irradiation using ferret data," In *Mechanisms and Control of Emesis* EDS A.L. Binchi, L. Grelot, A.D. Miller and G.L. King, Colloque INSERM/ John Libbey Eurotext Ltd, vol 223, 357.
- Nagayama H., Ooi J., Tomonari A., Iseki T., Tojo A., Tani K., Takahashi T.A., Yamashita N., and Shigetaka A., 2002. "Severe immune dysfunction after lethal neutron irradiation in a JCO nuclear facility accident victim," *Int. J. Hematol*, 76(2):157–164.
- Pellmar T.C., 2011. *Bone Marrow Niches in Hematopoiesis*. ARA/HS-TN-11-009-A, Applied Research Associates Technical Note, Arlington, VA.
- Qu Y., Jin S., Zhang A., Zhang A., Shi X., Wang J., and Zhao Y., 2010. "Gamma-Ray Resistance of Regulatory CD4⁺ CD25⁺ Foxp3⁺ T Cells in Mice," *Radiation Research*, 173(2):148–157.
- Shen S., DeNardo G.L., Jones T.D., Wilder R.B., O'Donnell R.T., and DeNardo S.J., 1998. "A preliminary cell kinetics model of thrombocytopenia after radioimmunotherapy," *J. Nucl. Med*, 39(7):1223–1229.
- Smirnova, O.A., 2010. *Environmental Radiation Effects on Mammals*. New York, NY: Springer New York.
- Wang X.S., Shi Q., Williams L.A., Mao L., Cleeland C.S., Komaki R.R., Mobley G.M., and Liao Z., 2010. "Inflammatory cytokines are associated with the development of symptom burden in patients with NSCLC undergoing concurrent chemoradiation therapy," *Brain Behav. Immun*, 24(6):968–974.
- Young, R.W., and Auton D.L., 1984. *The Defense Nuclear Agency Intermediate Dose Program: An overview. In Proceedings of the Psychology in the Department of Defense, Ninth Symposium*. TR-84-2; NTIS ADA141-043-0, edited by G. E. Lee and T. E. Ulrich. Colorado Springs: U.S. Air Force Academy, 85-89.
- Zukhbaya T.M., and Smirnova O.A., 1991. "An experimental and mathematical analysis of lymphopoiesis dynamics under continuous irradiation," *Health Phys*, 61(1):87–95.

APPENDIX A. ACRONYM LIST

BM	Bone Marrow
DNA	Deoxyribonucleic Acid
DTRA	Defense Threat Reduction Agency
ECs	Enterochromaffin Cells
ED ₅₀	Effective Dose in 50% of the population
EPD	Equivalent Prompt Dose
FL	Fluid Loss and electrolyte imbalance
FW	Fatigability and Weakness
GI	Gastrointestinal
GIM	Gut Injury Model
H	Homeostatic factor
HY	Hypotension
IB	Infection and Bleeding
IDP	Intermediate Dose Program
L	Lethal
LG	Lower Gastrointestinal
LPL	Lethal/Potentially-Lethal
M	Mitotic delay factor
MarCell	Marrow Cell
MLEs	Maximum Likelihood Estimates
MLT	Midline Tissue dose
NAS	Neuroactive Substance
P	Performance
PAIR	Proliferation and Intracellular Repair
PL	Potentially Lethal
Q	Damage
RBE	Relative Biological Effectiveness
RIPD	Radiation-Induced Performance Decrement
S/S	Signs/Symptoms
UG	Upper Gastrointestinal

THIS PAGE IS INTENTIONALLY LEFT BLANK.

**DISTRIBUTION LIST
DTRA-TR-12-47**

DEPARTMENT OF DEFENSE

DEFENSE TECHNICAL
INFORMATION CENTER
8725 JOHN J. KINGMAN ROAD,
SUITE 0944
FT. BELVOIR, VA 22060-6201
ATTN: DTIC/OCA

**DEPARTMENT OF DEFENSE
CONTRACTORS**

EXELIS, INC.
1680 TEXAS STREET, SE
KIRTLAND AFB, NM 87117-5669
ATTN: DTRIAC